JME

Journal of Mining & Environment,
Vol.6, No.2, 2015, 169-181.

3D stochastic rock fracture modeling related to strike-slip faults

M. Noroozi*, R. Kakaie and S.M.E. Jalali

School of Mining, Petroleum & Geophysics Engineering, Shahrood University of Technology, Shahrood, Iran

Received 8 June 2014; received in revised form 12 February 2015; accepted 22 February 2015
Corresponding author: mnoroozi.mine@gmail.com (M. Noroozi).

Abstract
Fault zones and fault-related fracture systems control the mechanical behaviors and fluid-flow properties of the Earth's crust. Furthermore, nowadays, modeling is being increasingly used in order to understand the behavior of rock masses, and to determine their characteristics. In this work, fault zones and fracture patterns are reviewed, and also comprehensive studies are carried out on the fracture geometry and density variations. A model to describe damage zones around the strike-slip faults is developed, in which the range of damage zone styles commonly found around strike-slip fault zones are shown. A computer code, named DFN-FRAC^{3D}, is developed for the two- and three-dimensional stochastic modeling of rock fracture systems in fault zones. In this code, the pre-existing and fault-related fractures are modeled by their respective probability distributions, and the joint density may be varied by the distance from the fault core. This work describes the theoretical basis and the implementation of the code, and provides a case study in the rock fracture modeling to demonstrate the application of the prepared code.

Keywords: *3D Stochastic Rock Fracture Modeling, Strike-Slip Faults, Fault-Related Fractures.*

1. Introduction

A rock mass comprises rock materials and discontinuities that include pores, fractures (joints), faults, and bedding planes. In most engineering applications, these discontinuities are the critical factors that determine the quality of rock masses such as the strength of rock structures or the flow characteristics of rock masses [1, 2]. In large scales, fault zones and fracture systems within fault damage zones (consisting of fault-related and pre-existing fractures) control the mechanics and fluid-flow properties of the Earth's crust [3]. Faults and fracture networks within fault damage zones are also the major decisive factors involved in the stability of rock slopes and underground openings in civil and mining engineering.

In spite of the importance of fault and damage zones in the mechanics and hydraulic properties of rock masses, it is impossible to map the fracture networks in fault damage zones in engineering scale accurately since accurate field measurement of a single discontinuity is difficult, and measurement of all discontinuities is impossible. Besides, there are always some random variations in the geometric properties of joints such as dip, dip direction, spacing, and persistence by virtue of the rock mass heterogeneous nature [4]. In practical applications, therefore, the only realistic approach is via a stochastic model that is formed from sparse data, which normally come from surveys of the analogues such as rock outcrops.

To generate the 2D and 3D fractures and fracture networks, in this work, a computer-code was developed based upon the general review of fracture patterns and the joint density variations in fault zones. In this code, the geometric properties of fault-related and pre-existing fractures are modeled by their respective probability distributions. Moreover, joint density may be varied by distance from the fault core according to an exponential or linear trend. This code, written using the C++ programming language, is able to represent the joint networks in different directions, and to generate digital outputs. The developed code is general with regard to design,

and the output can be exported for subsequent flows or mechanical analyses.

2. Fault damage zone

Fault zones, especially fault damage zones, show very different fracture geometries and patterns across a wide range of scales. Active fault zones are generally characterized by damage zones developed on either side of the fault, and an intervening fault core zone that contains the main slip surfaces [5, 6]. A damage zone, the volume of deformed wall rocks around a fault core, generally consists of fractures over a wide range of length scales and subsidiary faults [3] that result from the initiation and propagation of slip along faults [7]. In the case of a mature fault, the width of damage zone varies from decameters to kilometers [6, 8]. The width of damage zone is typically affected by the seismic faulting that occurs on the main fault planes [9]. In addition, the size of damage zone is dependent upon the lithologies that have been faulted, the deformation conditions, and the distribution of strain between the hanging wall and footwall [10]. In contrast, the fault core zone is generally concentrated in a narrow zone of around 0.5 to around 5 m in a width that lacks the primary cohesion of the host rocks [11, 12].

In the following sections, first of all, a general review is presented on the fault damage zone. Next, comprehensive studies are given on density variations *vs.* distance from the fault core and geometries of fault-related fractures.

2.1. Review of fault damage zone

Damage zones are divided into the tip damage, linking damage, and wall damage zones based on the position within and around a fault zone (Figure 1). A tip damage zone develops in response to the stress concentration at a fault tip [13]. Linking damage zones are caused by the interaction and linkage of fault segments in a relatively small region, and can develop a wide range of fracture patterns that depend on the nature of the interaction between the two fault segments. Wall damage zones result from the propagation of the modes II and III fault tips through a rock or from the damage associated with increase in the slip on a fault [5]. This section presents a model for damage zones around the strike-slip faults, as shown in Figure 2, which shows the range of damage zone styles that are commonly found around the strike-slip fault zones. It is acknowledged that any simple model, such as the model prepared in this work, cannot describe all of the complexities in the deformation that occurs around the faults.

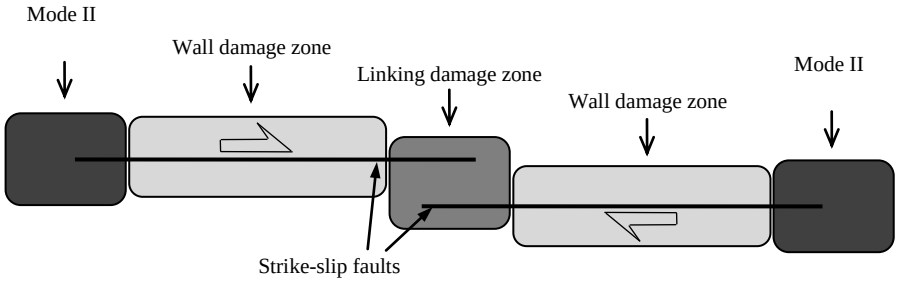

Figure 1. Schematic diagram for principal locations of damage zones around a strike-slip fault zone in map view [5].

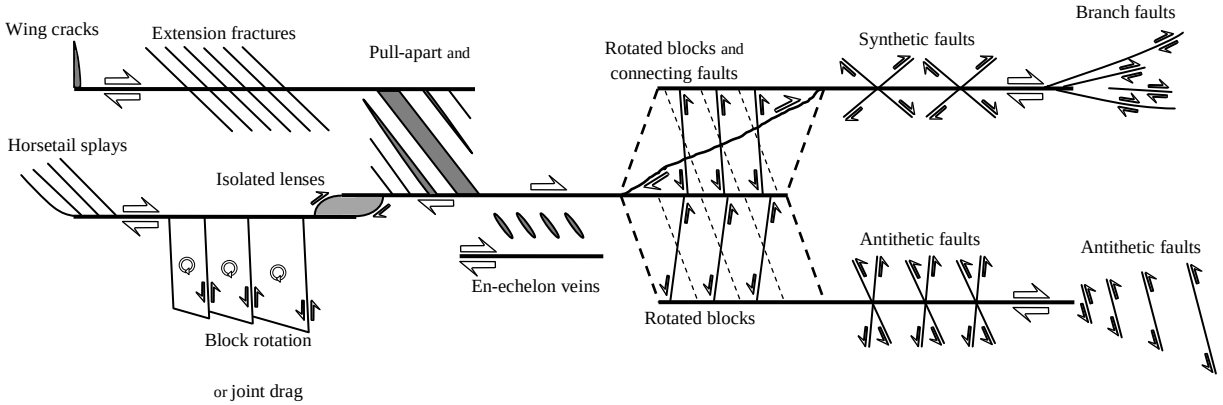

Figure 2. Schematic diagram sowing structures around strike-slip fault damage zones.

2.1.1. Tip damage zones

Tip damage zones can be sub-divided into four simple sub-divisions (Figure 2), including wing cracks, horsetail fractures, synthetic branch faults, and antithetic faults.

Wing cracks occur where there is a rapid decrease in slip at the fault tip. Horsetail fractures or pinnate fractures are geometrically and mechanically similar to wing cracks but they are finer and more closely spaced, with relatively low angles to the master faults. Synthetic branch faults have the same slip sense as the main fault, and may link with a neighboring fault segment [5]. Branch faults may combine with other structures in tip damage zones to produce complicated fracture patterns. Tip damage zones generally consist of several antithetic faults that splay out, increasing their length, and spacing away from the fault tip [8, 14].

2.1.2. Linking damage zones

Linking damage zones evolve between the interacting tips of adjacent faults [15]. Linking damage zones can be sub-divided into two sub-divisions (Figure 2), including extensional steps and contractional steps. Various types of developed structures in the extensional steps include the extension fractures, pull-aparts, rotated blocks, and strike-slip duplexes (Figure 2). The extension fractures are adjacent to the fault segments, and some link the two fault segments. Pull-aparts are a type of extension fractures that open-up between two fault segments due to increasing slip on the fault segments [16, 17]. Rotated blocks can occur in the extensional steps. The blocks rotate synthetically, with the rotation angle increasing as the fault slip increases. The strike-slip duplexes [18] or isolated lenses form at a fault step between two stepping fault segments [19].

Various types of developed structures in the contractional steps consist of the rotated blocks, connecting faults and strike-slip duplexes or isolated lenses (Figure 2).

Some of the faults within the rotated blocks (in the contractional steps between master faults) show a sigmoidal shape, implying a distributed simple shear within the step [20]. The connecting faults link two fault segments through a contractional overstep [16]. Veins, anti-thetic faults, and pressure solution seams also occur within the fault step. In the contractional steps, simple lenses are more common than the strike-slip duplexes [15].

2.1.3. Wall damage zones

A wall damage zone can be distributed along the whole trace of a fault. This damage zone can be sub-divided into three groups [5]: (1) wedge-shaped repeated damage zones, (2) long and relatively narrow damage zones, and (3) intensive damage zones in one wall of a fault.

Wedge-shaped damage zones are repeated along a fault trace, with the size of wedges generally increasing from the center to the tips of a fault. Wing cracks, extension fractures or veins occur in wall damage zones [14]. Cox and Scholz (1988) have suggest that the extension fractures generally form at around 45° to the master fault, although this angle varies considerably, with the angle depending on the fault type and stress system [17].

The en-echelon fractures within long, relatively narrow wall damage zones are interpreted as the primary antithetic faults or as the extension fractures that have been reactivated as antithetic faults (Figure 2).

Intense wall damage zones can result from frictional attrition as slip builds upon a fault [14]. This type of wall damage zone is asymmetric across the faults. Block rotation commonly occurs around large slip faults [21]. Antithetic faults are developed almost normal to the master fault, and the blocks rotate synthetically with respect to the master fault. Joint drags can also be developed in this type of damage zone (Figure 2).

In general, the patterns for damage zones depend on the 3D locations around the fault, stress perturbations that are controlled by the tip mode, amount of slip, and interaction between the segment faults.

Other factors are also likely to influence the nature of damage zones, including lithology, fluid pressure, and temperature. Damage zone patterns tend to become more complex during the evolution of damage zones. In general, any simple model cannot describe all the complexities in the deformation that occurs around faults.

2.2. Variation of joint density in fault damage zones

Quantitative studies of damage zones commonly involve determining the density of fractures (usually from line or plane counting) as a function of distance from the fault core. An exponential decrease with distance from the fault core is commonly shown by the macro-fractures (meso-scale features that may be readily identified in the field) and micro-fractures (measured from orientated thin sections) for low-porosity rocks [3, 7, 22, 23]. This relationship may exist in high porosity sandstones, although, in some cases, micro-fractures in damage zones in high porosity sandstones show no observable change in the micro-fracture density surrounding faults [24].

As a whole rule, a maximum micro-fracture density is often attained immediately adjacent to the fault core that is independent from the fault displacement. In addition, decrease in joint density with distance from the fault core may be according to a linear trend or an irregular fashion. Field investigation results in the fault zone width along the strike-slip active faults of the Arima-Takatsuki tectonic line (ATTL) and the Rokko-Awaji fault zone (RAFZ) in the south-west of Japan have shown that the decreasing trend of joint density with distance from the fault is linear in some profiles, and irregular elsewhere [12].

3. Stochastic fracture system modeling associated with faults

For a realistic rock mass modeling, location of joints in the modeling volume should be simulated in a way that its probability distribution is similar to the actual joints in the rock mass. 3D stochastic joint network modeling is the most optimal choice to simulate the probability nature of joint geometric properties. Early interest in the mentioned approach was associated with the structure design in jointed rocks, the evaluation and construction of underground repositories for the safe storage and disposal of hazardous wastes, underground water transport through aquifers in hydrogeological engineering, and movement of oil and gas in hydrocarbon reservoirs [25- 27]. Nowadays, a few commercial softwares such as FRACMAN, GEOFRAC, and SIMBLOCK are available for the stochastic modeling of rock masses that are used for the rock mechanics research, particularly in flow-modeling through jointed rock mass and determination of its permeability.

The geologic stochastic models developed at MIT [28, 29] can be considered as the initially prepared models in this field. Afterwards, further research has been carried out on the basic fracturing processes to develop the hierarchical fracture geometry model, to model fluid-flow and slope stability analysis, each of which includes some geometric and mechanical properties of the joints [30-38]. In recent years, further developments have been obtained in the 2D and 3D stochastic models in order to examine the effects of considering, or not considering, the correlation between distributions of fracture apertures and fracture trace lengths in the hydro-mechanical behavior of fractured rocks [27, 39, 40].

3.1. General approach

In stochastic modeling, the general approach is to treat locations, persistence (size), orientation, and other properties of the joints as random variables with inferred probability distributions. These distributions supply the basis of the stochastic occurrence. Then the rock joint model can be constructed using the Monte Carlo simulation method.

The first stage of the modeling process is to collect the discontinuity data for statistical analysis. The most common measurement technique is by scanlines, or window surveys, of rock outcrops or excavated rock surfaces [41]. If drill cores are available, scanlines and/or window surveys can also be applied to the core samples

[37]. Additional data can be obtained along the borehole using down-the-borehole camera, geophysical logging [42], and the useful remote methods for mapping exposures such as photogrammetry and laser-scanning [43]. Measurements of discontinuity traces at rock exposures are subjected to orientation, truncation, censoring, and size biases [37, 44]. Therefore, the 2D data requires correction before using in the 3D modeling [45].

The joints are grouped in joint sets, which are identified from the statistics of the measured data and the geologic history of the region. The primary fractures that originate from the intact rock are combined into independent sets. Each set is modeled separately, and the final simulation is the simple combination of all the independently simulated sets. The joints that open as secondary, tertiary, etc. within a previously jointed rock mass, and are related to the primary ones with respect to their location, orientation, size, and other geometric characteristics, are grouped into dependent sets. The correlations can be modeled either by a hierarchical model [36, 46] or by the plurigaussian simulation technique [47].

A fracture set is characterized by the following four parameters:

a) Fracture center location

b) Probability density function (PDF) of variation in the fracture plane orientations

c) Mean orientation of fracture set

d) Fracture intensity

In the current version of the model presented in this work, the joints were convex polygonal planar objects of discontinuous rock, randomly oriented and located in 3D spaces. In this work, the C++ language was used to develop the computer model. In the model, poisson plane and line stochastic processes were incorporated together. Then a joint set was generated in the modeling space around fault by applying a sequence of five stochastic processes, as follow:

- First process: a homogeneous Poisson network of planes in space.
- Second process: sub-division of each plane into a jointed region and its complementary region of intact rock by a homogeneous Poisson line network.
- Third process: non-homogeneous polygon marking procedure on created polygon in the previous step based on shape and size.
- Fourth process: defining zones within the modeling volume, using the perpendicular distance from one side of fault and marking the polygons located in the zones, retained from the previous process, with a certain probability that can vary from zone to zone. This process provides a means of modifying the fracture intensity (P_{32}) in different regions of the modeling volume.
- Fifth process: random shifting of the polygons that were marked as jointed in the vicinity of their original position.

The fracture set was generated in a modeling volume. In the first process, distance of the i^{th} stochastic fracture from the global origin was generated according to an exponential distribution with intensity μ. The process of fracture set generation was a Poisson plane process. This process has an unknown parameter: the number of planes to be generated. This number is related to the intensity of fracturing. A random sub-division of the planes, generated by the primary process, into a fractured region, and its complementary region of intact rock is accomplished by a Poisson line tessellation on every plane. The Poisson lines are defined by an angle α uniformly generated between zero and 2π, and a distance Di that is the sum of n distances dDi, generated according to an exponential distribution with intensity λ. The ordered distances Di from the origin to the Poisson lines form a Poisson point process. The third process is generated by the fracture sets with specific shape and size. Only polygons with shapes similar to the shapes of natural fractures remain. A polygon has a suitable shape, and is considered as a fracture, if it has the following conditions: a) the polygon has at least four vertices; b) all angles are at least 60 degrees; c) the polygon elongation is not more than the permitted value. A polygon is retained with probability P = 1.0, if it has an appropriate shape, and discarded otherwise. The fourth process is described in details in section 3.3. In the fifth stochastic process, translation is performed in the frame of reference of the fracture plane. Translation is accomplished by assigning a non-zero coordinate z into the center and the vertices of a polygon and hence to the entire polygon.

Fracture system, including fracture sets, is generated with reiteration of the presented processes. A fracture system is represented through super-position of fracture sets in a 3D space. The model building algorithm for a joint set is shown in Figure 3.

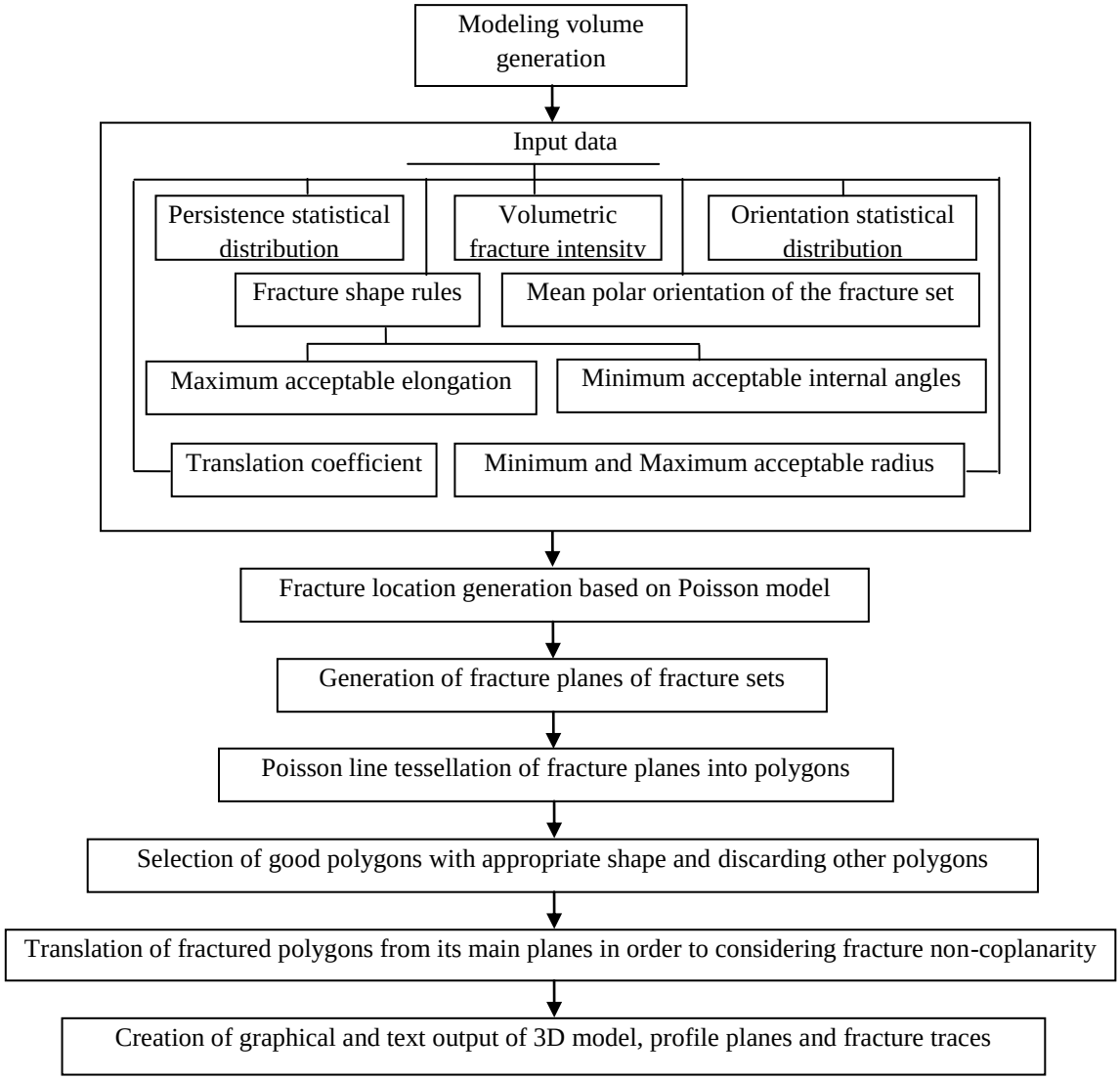

Figure 3. Presented method algorithm.

3.2. Input parameters

The main inputs required for construction of the 3D stochastic model are as follow:

3.2.1. Fracture location generation model

Simulation of joint locations is the first step in simulating joint networks, and is usually modeled separately from other fracture properties. In fact, in nature, fractures are distributed according to some forms of spatial models, and are generally associated with the geological process that caused their formation. For instance, the intensity of fractures is often observed in the cluster around the key structures such as faults, with a diminishing intensity with distance from the fault. An alternative, is the observation that fractures often tend to clump together [48].

The most common approach to produce the location of joints is to use a single point, usually the center of the joint. Geo-statistics or a random point process can then be used to model the spatial distribution of the joints. The point process model, parametric or non-parametric, may be a simple Poisson model or one of a number of non-homogeneous models including inhomogeneous, cluster, and Cox models. In the model presented in this work, the fracture location was modeled by the Poisson point process.

3.2.2. Volumetric fracture intensity

Volumetric fracture intensity, known as P_{32} (fracture area/unit volume), which is an intrinsic rock mass property, can be inferred from the 1D and 2D data available from boreholes and mapping, using a simulated sampling methodology. Volumetric fracture intensity is scale-independent, and as a volumetric parameter, its direction is also independent. The preferred

method of controlling fracture intensity is through the direct comparison between the intensities of the observed and simulated fractures [49].

3.2.3. Fracture shape

Fracture mechanics suggest that in a homogeneous rock, the general shape of an isolated fracture is elliptical, as it is assumed in the Baecher model [28]. However, as the rock is generally heterogeneous, perfectly elliptical fractures are unlikely to be formed. Dershowitz (1984) has noted, moreover, that the observed fractures are generally polygonal due to terminations of the fractures at the intersections with other fractures. In the presented model, fracture shapes were assumed to be polygons with at least four vertices and maximum permitted elongation.

3.2.4. Fracture orientation

Fracture orientation similar to the fracture intensity is generally defined using either borehole imaging data, face mapping or to use advanced photogrammetric methods. Processing the fracture orientation data allows it to be organized into distinct fracture sets with defined statistical properties. In view of its simplicity and flexibility, the Fisher distribution provides a valuable model to evaluate the discontinuity orientation data [34]. Possible distributions in the model presented in this work include constant (deterministic), uniform, partial uniform, and Fisher distributions, according to equations 1 and 2.

$$Uniform: f(x) = \begin{cases} \dfrac{1}{b-a} & a \le x \le b \\ 0 & otherwise \end{cases} \quad (1)$$

$$Fisher: f(x) = \frac{K \sin\theta \, e^{K\cos\theta}}{e^{K} - e^{-K}} \quad (2)$$

Where K is a constant, controlling the shape of the distribution.

3.2.5. Fracture size (persistence)

Many existing discrete fracture modeling methods assume fractures to be infinite in length, resulting in an erroneous definition of block geometry. Besides, there are very few published 3D fracture surveys [50]. Therefore, in practice, the sizes of 3D fractures are assumed to have similar statistical properties to those obtained in the 2D surveys [27]. Commonly, three basic forms of the true trace length distribution, negative exponential, lognormal, and gamma, are used to model the data derived from the 2D fracture mapping surveys [30, 34, 37, 41, 51]. In the model presented in this work, fracture sizes were fitted on these distributions, based on the following equations:

$$Negative\ \text{exponential}: f(l) = \gamma e^{-\gamma l} \quad (3)$$

$$Lognormal: f(l) = \frac{1}{l\sigma\sqrt{2\pi}} \exp\left(-\frac{[\ln(l) - \mu]^2}{2\sigma^2}\right) \quad (4)$$

$$Gamma: f(l) = \frac{\beta^{\alpha}}{\Gamma(\alpha)} l^{\alpha-1} e^{-\beta l} \quad (5)$$

In which γ is the intensity parameter; μ and σ are, respectively, the mean and standard deviations of trace length sample; α and β are the distribution parameters; and Γ is the gamma function.

3.3. Generation of fracture system associated with faults

Fracture systems associated with crustal faults include primary faults and numerous secondary fracture sets. Creation of new fractures often changes the local principal stress directions in the vicinity of primary faults. Numerous secondary, tertiary, etc. faults, and new joint sets are formed between and near the primary faults that have a specific patterns. Dip and strike of these joints are usually constant. Joint spacing can be considered to be constant or on an exponential trend. Joint systems related to the fault can be simulated by measuring the joint properties on the field. These fault-related fracture systems are added to the pre-existing fracture systems measured outside the fault damage zone.

Firstly, the pre-existing fractures are generated. The geometric properties of these fracture sets, outside the fault damage zones, are measured and modeled. Then the fault-related fracture sets are established. The geometric properties of these fracture sets within the fault damage zones are measured and modeled. After determining the mean pole orientation, the variation of fracture orientations in a dependent set can be considered as constant or can be modeled with uniform, partial uniform or Fisher PDF. The fracture sizes can also be fitted on specified distributions such as lognormal, exponential or gamma.

In the model presented in this work, the probability of marking a polygon as a fractured one is a function of the distance from the local faults. To obtain different fracture intensities of a fracture set in different portions V_1, V_2 …, V_i of

the modeling volume V, first, we have to calculate the different probabilities P_1, P_2 …, P_i. Volume V_i may be defined in terms of the distances from a fault face. Within every zone i, the zone probability P_i is constant but that constant is different in different zones. The polygon j in zone i is retained with probability P_i, and is discarded with probability 1 - P_i, where $0 < P_i \leq 1$.

As mentioned in the previous sections, joint density variations decrease with distance from the fault core, according to an exponential or linear trend. In each size interval from the fault face, i.e. zone 1 … zone i, the polygons generated by the model are selected as fractures with probability P_i.

The probability P_i in region V_i is calculated, as follows.

$$P_i = \frac{P_{32,i}}{P_{32,\max}} \quad (6)$$

Generally, fracture intensity is the highest value in regions adjacent to the fault, and the maximum fracture intensity ($P_{32,max}$) is measured in these regions. The fracture intensity in zone i ($P_{32,i}$) is obtained using the fracture intensity function *vs.* distance from the fault (Figure 4).

The translation procedure of the fifth process of the model can be applied to avoid the co-planarity of fault-related fractures.

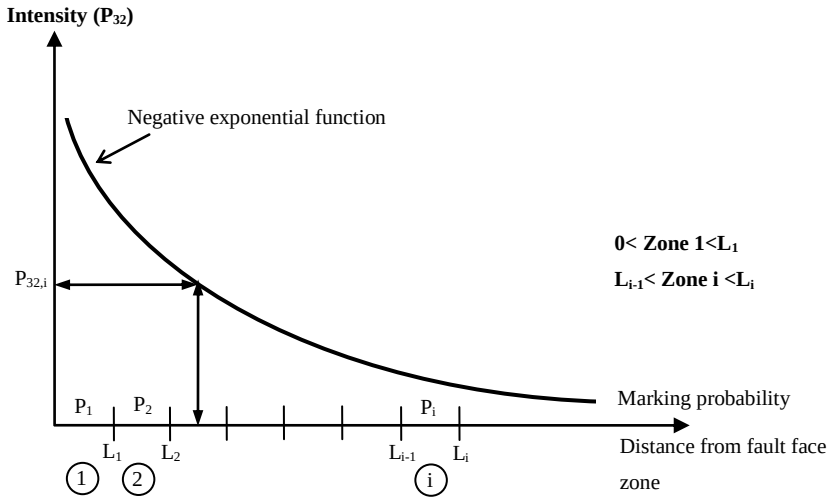

Figure 4. Definition of fracture zones and zone marking with probability P_i in region V_i.

4. Case study

In order to test the implementation of the presented model, the Lorestan Rudbar dam was selected for a study on the generation of fault-related fractures. The project was undertaken in the Lorestan Province, 100 kilometres from the southern boundary of Aligoodarz, and on the way to Rudbar river. Reverse or thrust faults, which are the main tectonic factors in the area, make the rocks appear broken-down. The faults are of great variety because of being located along Zagros. In this study, the FF.1 fault zone of the right wall of dam was chosen for scan-line mapping (Figure 5). To qualitatively assess the spatial distribution and width of damage zones and related deformation structures, first, field measurement of the fracture density was performed. Fractures that were visible to the naked eye in the field were counted within an area of 1 m^2 using a square frame (1 × 1 m) with grid lines at 10-cm intervals. The fractures that intersected each grid line were counted, and the total number of fractures counted in the 1 m^2 frame was defined as the fracture density (Figure 6). The measurement results were plotted as fracture density *vs.* distance from the fault (Figure 7). The fracture density varies from 9 fractures per unit area at the site located far from the main fault (regarded as part of the host-rock fracture density) to 27 fractures per unit area at the site located close to the main fault.

Based on the collected data from the scan-line mapping, the appropriate data required for the statistical studies was obtained from discriminating each joint set and specifying its related features such as dip, dip direction, spacing, and persistence. Then the distribution functions of these surveyed joint sets were determined. The geometrical properties of joint sets and the parameters of the corresponding probability distribution functions are presented in Table 1.

Table 1. Geometrical properties and parameters of PDFs of surveyed joint sets.

Joint set orientation (Dip/DDir)	Fisher constant (K)	Trace length distribution parameters				
		Distribution function	Scale parameter (σ)	Location parameter (μ)	Mean	Standard Deviation
1 (56/141)	19.9	lognormal	0.937	0.121	2.42	2.51
2 (78/019)	22.67	lognormal	0.858	-0.512	0.95	1.21
3(62/319)	20.58	lognormal	0.819	-0.624	0.88	1.38

Figure 8 illustrates the varying fracture intensities with increasing distance from the FF.1 fault, generated with the prepared computer code, DFN-FRAC^{3D}, that implemented the 3D stochastic model. Figure 8b shows the relative locations of the fault, and the two outcrop planes: vertical and horizontal. Since strike-slip faults are steeply dipping planes of shear failure, and are often vertical, the fault plane is modeled as vertical plane in the current version of the DFN-FRAC^{3D}. Figures 8c and 8d illustrate the trace outcrops of the fracture network on the horizontal and vertical outcrop planes, respectively. The modeling volume, currently implemented in the developed code, was enclosed between four vertical planes at $X = X_m$, $X = -X_m$, $Y = Y_m$, and $Y = -Y_m$, and two horizontal planes at $Z = 0$ and $Z = Z_m$.

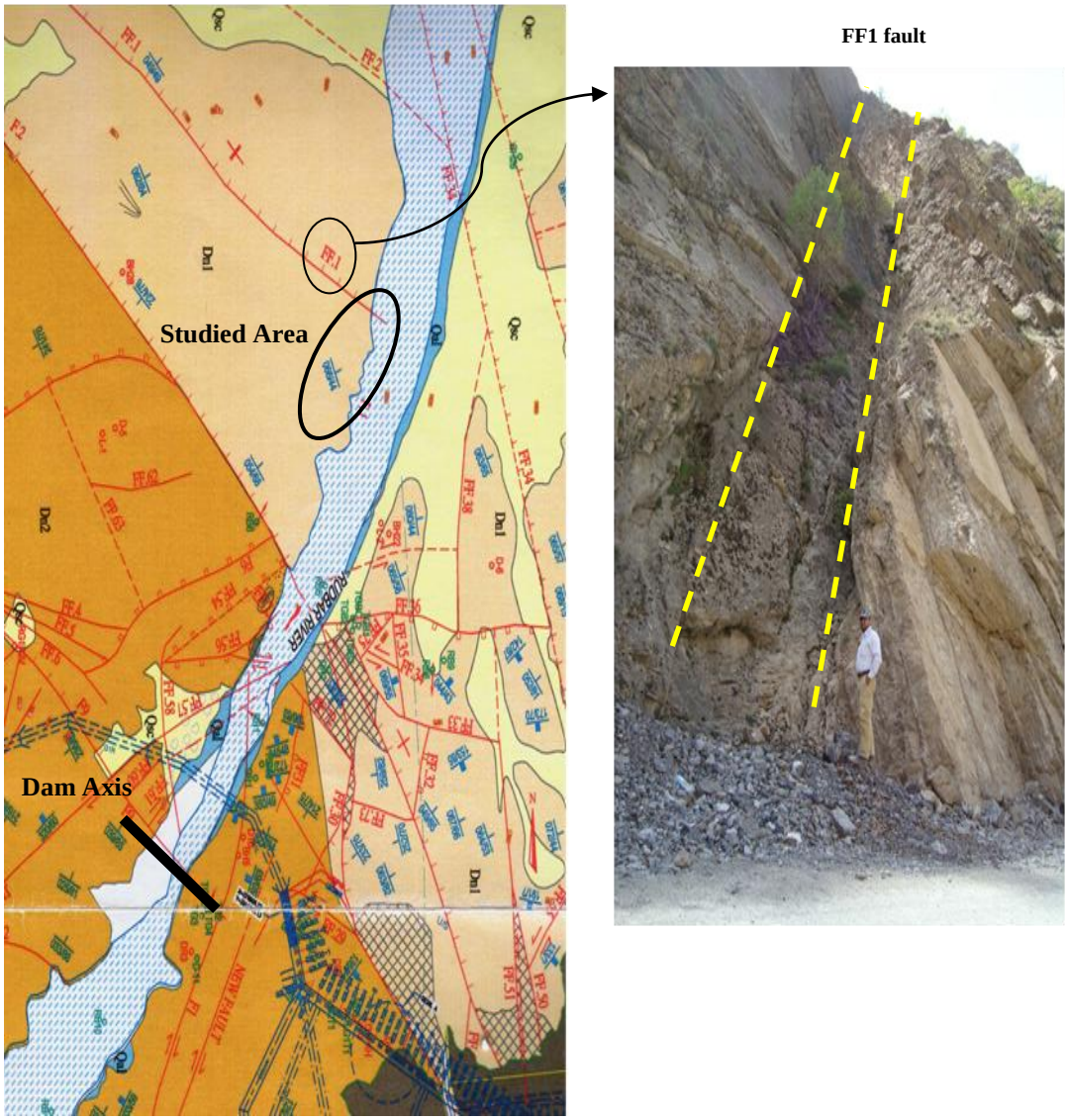

Figure 5. Geological map of studied region.

Figure 6. Joint density measurements.

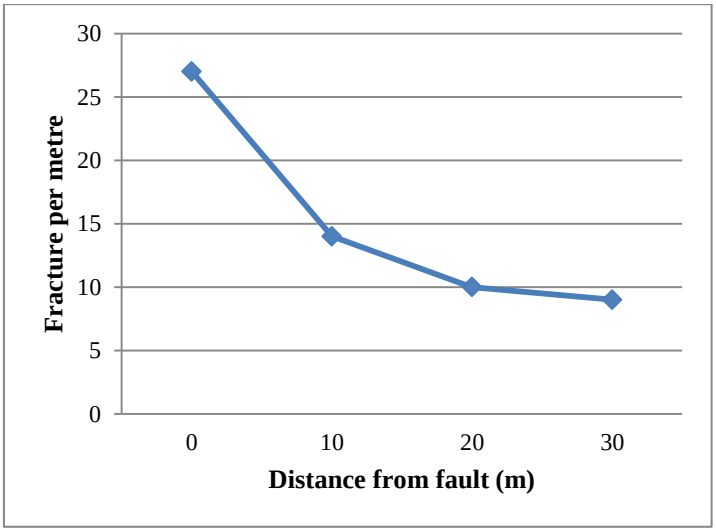

Figure 7. Spatial variations in fracture density with increasing distance from FF.1 fault.

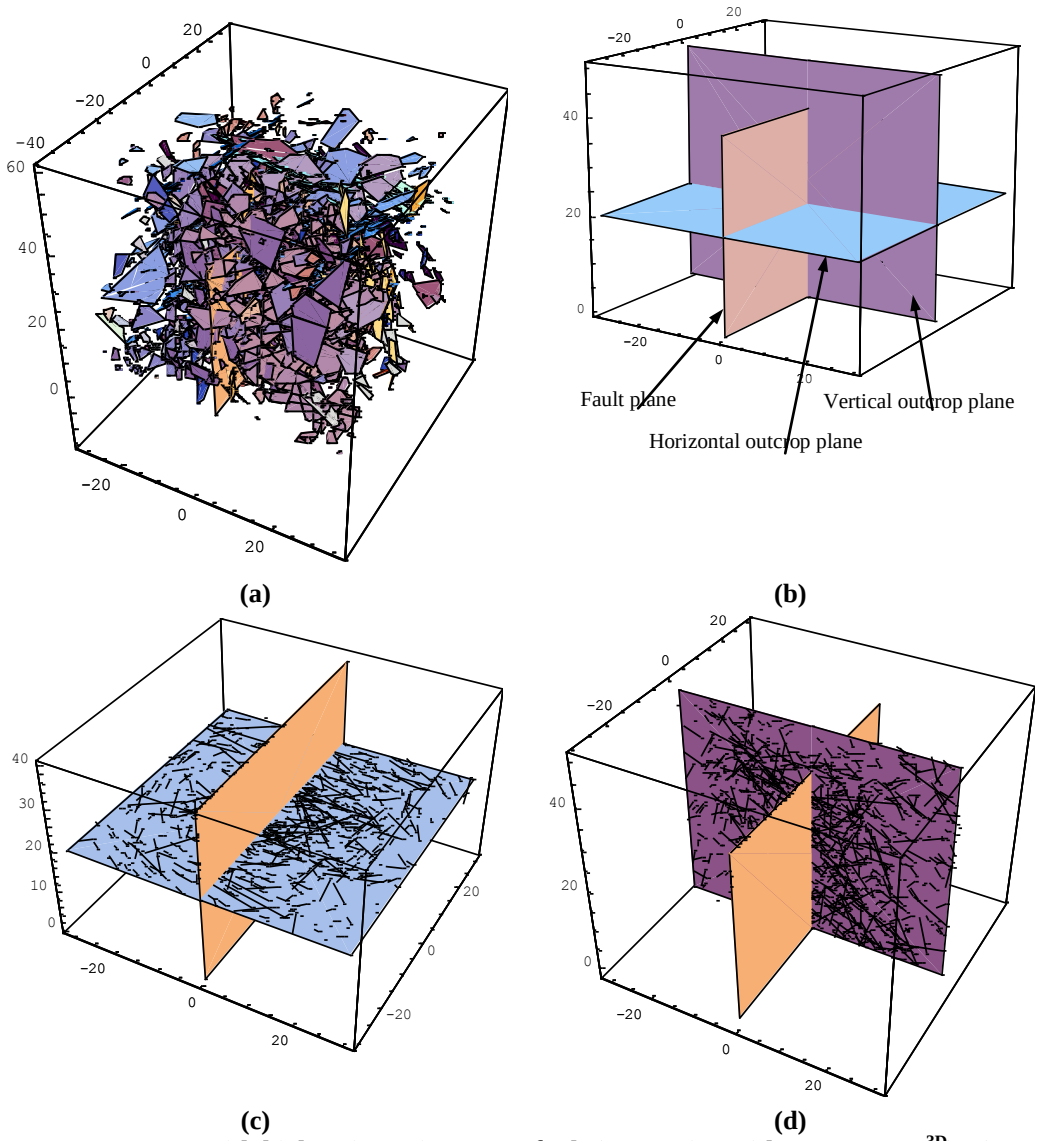

Figure 8. Fracture system with highest intensity near a fault (generation with DFN-FRAC^{3D}): a) 3D fracture system; b) fault and outcrop planes; c) horizontal trace outcrop; d) vertical trace outcrop.

5. Conclusions

In this work, based on comprehensive studies on the fault zones, fracture patterns, and fracture density variations in fault damage zones, a model was developed for the damage zones around the strike-slip faults. Moreover, this paper describes a computer-code, DFN-FRAC^{3D}, for the stochastic simulation of fractures around faults in two and three dimensions. In this code, joint density is modeled as a function of distance from the fault core, according to an exponential or linear trend. This code has an ability to display joint network in different directions, create a 2D section, and present joint traces in the desired directions and locations. A case study for the FF.1 fault of the right wall of Lorestan Roodbar dam showed that the developed computer code can, very well, be used for modeling a faulted rock mass and its fault-related fractures in reality. The results obtained from this work can be a useful input for hydraulic behavior studies of faulted rock masses. This code can also be improved by considering non-vertical fault planes (with desired direction) in modeling of the thrust faults.

References

[1]. Le Garzic, E., L'Hamaide, T., Diraison, M., Géraud, Y., Sausse, J., Urreiztieta, M., Hauville, B. and Champanhet, J. M. (2011). Scaling and geometric properties of extensional fracture systems in the proterozoic basement of Yemen. Tectonic interpretation and fluid flow implications, Journal of Structural Geology. 33: 519- 536.

[2]. Gumede, H. and Stacey, T. R. (2007). Measurement of typical joint characteristics in South

African gold mines and the use of these characteristics in the prediction of rock falls, The Journal of the Southern African Institute of Mining and Metallurgy. 107: 335- 344.

[3]. Faulkner, D. R., Jackson, C. A. L., Lunn, R. J., Schlische, R. W., Shipton, Z. K., Wibberley, C. A. J. and Withjack, M. O. (2010). A review of recent developments concerning the structure, mechanics and fluid flow properties of fault zones, Journal of Structural Geology. 32: 1557- 1575.

[4]. Hoek, E. T. (1998). Reliability of the Hoek–Brown estimates of rock mass properties and their impact on design, Int J Rock Mech Min Sci. 35: 63- 68.

[5]. Kim, Y. S., Peacock, D. C. P. and Sanderson, D. J. (2004). Fault damage zones, Journal of Structural Geology. 26 (3): 503- 517.

[6]. Takagi, H., Takahashi, K., Shimada, K., Tsutsui, K., Miura, R., Kato, N. and Takizawa, S. (2012). Integrated estimates of the thickness of the fault damage zone in granitic terrain based on penetrative mesocracks and XRD analyses of quartz, J Struct Geol. 35: 64- 77.

[7]. Vermilye, J. M. and Scholz, C. H. (1998). The process zone: a microstructural view of fault growth, Journal of Geophysical Research. 103: 12223- 12237.

[8]. McGrath, A. G. and Davison, I. (1995). Damage zone geometry around fault tips, Journal of Structural Geology. 17: 1011- 1024.

[9]. Lin, A., Ren, Z. and Kumahara, Y. (2010). Structural analysis of the coseismic shear zone of the 2008 Mw 7.9 Wenchuan earthquake, China, J Struct Geol. 32: 781- 791.

[10]. Peacock, D. C. P. (2002). Propagation, interaction and linkage in normal fault systems, Earth-Science Reviews. 58: 121- 142.

[11]. Mitchell, T. M., Ben-Zion, Y. and Shimamoto, T. (2011). Pulverized fault rocks and damage asymmetry along the Arima-Takatsuki Tectonic Line, Japan, Earth Planet Sci Lett. 308: 284- 297.

[12]. Lin, A. and Yamashita, K. (2013). Spatial variations in damage zone width along strike-slip faults: An example from active faults in southwest Japan, Journal of Structural Geology. 57: 1- 15.

[13]. Cowie, P. A. and Scholz, C. H. (1992). Physical explanation for the displacement-length relationship of faults, using a post-yield fracture mechanics model, J Struct Geol. 14: 1133- 1148.

[14]. Kim, Y. S., Peacock, D. C. P. and Sanderson, D. J. (2003). Strike-slip faults and damage zones at Marsalforn, Gozo Island, Malta, Journal of Structural Geology. 25: 793- 812.

[15]. Kim, Y. S., Andrews, J. R. and Sanderson, D. J. (2001). Secondary faults and segment linkage in strike-slip fault systems at Rame Head, southern Cornwall, Geoscience in South-West England. 10: 123- 133.

[16]. Peacock, D. C. P. and Sanderson, D. J. (1995). Strike-slip relay ramps, Journal of Structural Geology. 17: 1351-1360.

[17]. Peacock, D. C. P. and Sanderson, D. J. (1995). Pull-aparts, shear fractures and pressure solution, Tectonophysics. 241: 1- 13.

[18]. Woodcock, N. H. and Fischer, M. (1986). Strike-slip duplexes, Journal of Structural Geology. 8: 725-735.

[19]. Kim, Y. S., Andrews, J. R. and Sanderson, D. J. (2001). Reactivated strike-slip faults: examples from north Cornwall, UK, Tectonophysics. 340: 173- 194.

[20]. Ramsay, J. G. and Huber, M.I. (1983). The Techniques of Modern Structural Geology, Volume 1, Strain Analysis, Academic Press, London, 307 p.

[21]. Dibblee, T. W. (1977). Strike-slip tectonics of the San Andreas Fault and its role in Cenozoic basin evolution, American Association of Petroleum Geologists Reprint. 28: 159- 172.

[22]. Wilson, J. E., Chester, J. S. and Chester, F. M. (2003). Microfracture analysis of fault growth and wear processes, Punchbowl Fault, San Andreas System, California, Journal of Structural Geology. 25 (11): 1855- 1873.

[23]. Mitchell, T. M. and Faulkner, D. R. (2009). The nature and origin of off-fault damage surrounding strike-slip fault zones with a wide range of displacements: a field study from the Atacama fault system, northern Chile, J Struct Geol. 31: 802- 816.

[24]. Shipton, Z. K. and Cowie, P. A. (2001). Damage zone and slip-surface evolution over μm to km scales in high-porosity Navajo sandstone, Utah, Journal of Structural Geology. 23 (12): 1825- 1844.

[25]. Dershowitz, W. S. (1992). The role of the Stripa Phase 3 Project in the development of practical discrete fracture modeling technology, In Proc., Fourth International NEA/SKB Symposium, Stockholm, Paris. 231- 258.

[26]. Rogers, S. F., Moffitt, K. M. and Kennard, D. T. (2006). Probabilistic slope and tunnel block stability analysis using realistic fracture network models, In Proc. 41st U.S. Symposium on Rock Mechanics, Golden, CO. ARM, VUSRMS. 1006- 1052.

[27]. Xu, C. and Dowd, P. (2010). A new computer code for discrete fracture network modeling, Computers & Geosciences. 36: 292- 301.

[28]. Baecher, G. B., Einstein, H. H. and Lanney, N. A. (1977). Statistical description of rock properties and sampling, In: Proc. 18th U.S.symposium on rock mechanics. Golden: Colo. Sch. Mines Press. 1- 8.

[29]. Veneziano, D. (1978). Probabilistic models of joints in rock, Research report. Department of Civil and Environmental Engineering, Massachusetts Institute of Technology, Cambridge, MA.

[30]. Baecher, G. B. (1983). Statistical analysis of rock mass fracturing, Journal of Mathematical Geology. 15: 329- 347.

[31]. Einstein, H. H., Veneziano, D., Baecher, G. B. and O'Reilly, K. J. (1983). The effect of discontinuity persistence on rock slope stability, International journal of rock mechanics and mining sciences & geomechanics abstracts. 20 (5): 227- 236.

[32]. Dershowitz, W.S. (1984). Rock joint systems, PhD Thesis. Massachusetts Institute of Technology, Cambridge, MA.

[33]. Dershowitz, W. S. and Einstein, H. H. (1988). Characterizing rock joint geometry with joint system models, Rock Mechanics and Rock Engineering. 21: 21- 51.

[34]. Priest, S. D. (1993). Discontinuity Analysis for Rock Engineering, Published by Chapman & Hall, 2-6 Boundary Row, London SE1 8 HN.

[35]. Kulatilake, P. H. S. W., Wathugala, D. N. and Stephansson, O. (1993). Stochastic three dimensional joint size, intensity and system modeling and a validation to an area in Stripa Mine, Sweden. Soils foundations. 33 (1): 55- 70.

[36]. Ivanova, V., Xiaomeng, Y., Veneziano, D. and Einstein, H. H. (1995). Development of stochastic models for fracture systems, Rock Mechanics, Daemen & Schultz (eds) Balkema, Rotterdam. ISBN: 90 5410 552 6.

[37]. Zhang, L. and Einstein, H.H. (2000). Estimating the Intensity of Rock Discontinuities, International Journal of Rock Mechanics and Mining Science. 37: 819- 837.

[38]. Kulatilake, P. H. S. W., Park, J. and Um, J. (2004). Estimation of rock mass strength and deformability in 3-D for a 30 m cube at a depth of 485 m at Aspo Hard Rock Laboratory, Geotechnical and Geological Engineering. 22: 313-330.

[39]. Baghbanan, A. and Jing, L. (2008). Hydraulic properties of fractured rock masses with correlated fracture length and aperture, International Journal of Rock Mechanics & Mining Sciences. 44: 704- 719.

[40]. Bang, S. H., Jeon, S. and Kwon, S. (2012). Modeling the hydraulic characteristics of a fractured rock mass with correlated fracture length and aperture: application in the underground research tunnel at Kaeri, Nuclear engineering and technology. 44 (6): 639- 652.

[41]. Kulatilake, P. H. S. W., Um, J., Wang, M., Escandon, R. F. and Varvaiz, J. (2003). Stochastic fracture geometry modeling in 3-D including validations for a part of Arrowhead East Tunnel, California, USA, Eng Geol. 70: 131- 155.

[42]. Ozkaya, S. I. and Mattner, J. (2003). Fracture connectivity from fracture intersections in borehole image logs, Computers & Geosciences. 29: 143- 153.

[43]. Coggan, J. C., Wetherelt, A. and Flynn, Z. N. (2006). Modelling fractured rock masses in underground spaces, Tunnels and Tunnelling International. 38- 41.

[44]. Kulatilake, P. H. S. W. and Wu, T. H. (1984). Sampling bias on orientation of discontinuities, Rock Mech Rock Eng. 17 (4): 215- 232.

[45]. Fouche, O. and Diebolt, J. (2004). Describing the geometry of 3D fracture systems by correcting for linear sampling bias, Mathematical Geology. 36 (1): 33- 63.

[46]. Lee, J. S., Veneziano, D. and Einstein, H. H. (1990). Hierarchical fracture trace model, In: Proc. of the 31th US Rock Mechanics Symposium, Balkema, Rotterdam. 261- 268.

[47]. Dowd, P. A., Xu, C., Mardia, K. V. and Fowell, R. J. (2007). A comparison of methods for the simulation of rock fractures, Mathematical Geology. 39: 697- 714.

[48]. Rogers, S. F., Kennard, D. K., Dershowitz, W. S. and Vanas, A. (2007). Characterising the in situ fragmentation of a fractured rock mass using a discrete fracture network approach. Rock Mechanics: Meeting Society's Challenges and Demands - Eberhardt, Stead & Morrison (eds) Taylor & Francis Group, London, ISBN: 978-0-415-44401-9.

[49]. Dershowitz, W. S., Lee, G., Geier, J., Foxford, T., LaPointe, P. and Thomas, A. (2004). FracMan, interactive discrete feature data analysis, geometric modeling, and exploration simulation, user documentation Seattle: Golder Associates Inc.

[50]. Dowd, P. A., Martin, J., Mardia, K. V., Fowell, R. J. and Xu, C. (2009). A three-dimensional fracture network data set for a block of granite, International Journal of Rock Mechanics and Mining Sciences. 46 (5): 811- 818.

[51]. Zadhesh, J., Jalali, S. E. and Ramezanzadeh, A. (2013). Estimation of joint trace length probability distribution function in igneous, sedimentary, and metamorphic rocks, Arab J Geo sci. DOI: 10.1007/s12517-013-0861-1.

توسعه مدل تصادفی سه‌بعدی شبکه درزه‌ها با در نظر گرفتن گسل‌های امتداد لغز

مهدی نوروزی*، رضا کاکائی و سید محمد اسماعیل جلالی

دانشکده مهندسی معدن، نفت و ژئوفیزیک، دانشگاه صنعتی شاهرود، ایران

ارسال ۲۰۱۴/۶/۸، پذیرش ۲۰۱۵/۲/۲۲

* نویسنده مسئول مکاتبات: mnoroozi.mine@gmail.com

چکیده:

نواحی گسلی و سیستم‌های درزه وابسته به آن، ویژگی‌های مکانیکی و هیدرولیکی پوسته زمین را کنترل می‌کنند. از طرفی، امروزه به‌منظور تعیین دقیق ویژگی‌های توده سنگ و بهبود درک رفتار آن، مدل‌سازی توده سنگ به‌طور فراگیری بکار برده می‌شود. در این مقاله، بررسی جامعی بر روی ناحیه گسلی، الگوهای درزه و ساختارهای داخلی آن انجام‌شده است. همچنین مطالعات جامعی در خصوص تغییرات چگالی و هندسه درزه‌ها در این مقاله صورت گرفته است. مدلی برای توصیف نواحی تخریب توسعه‌یافته در اطراف گسل‌های امتدادلغز ارائه‌شده که در آن دامنه حالت‌های نواحی تخریب که به‌طور معمول در اطراف گسل‌های امتدادلغز اتفاق می‌افتد، نشان داده‌شده است. برنامه‌ای کامپیوتری به نام $DFN\text{-}FRAC^{3D}$ برای مدل‌سازی تصادفی دوبعدی و سه‌بعدی سیستم‌های درزه در نواحی گسلی توسعه داده شد. در این برنامه درزه‌های موجود و درزه‌های وابسته به گسل توسط توزیع‌های احتمال مربوطه مدل‌سازی می‌شوند و چگالی درزه با فاصله از هسته گسل می‌تواند به‌طور نمایی یا خطی تغییر کند. در این مقاله اصول تئوری و کاربرد برنامه توصیف می‌شود و یک مورد مطالعاتی برای نشان دادن کاربرد عملی آن ارائه‌شده است.

کلمات کلیدی: مدل‌سازی تصادفی سه‌بعدی درزه‌ها، گسل‌های امتدادلغز، درزه‌های وابسته به گسل.